

Enhanced scratch resistance of self-assembled silica nanoparticle anti-reflection coatings

Jonathan S. Metzman^{1*}, Guanyu Wang, John R. Morris, James R. Heflin^{2*}

¹Department of Materials Science and Engineering, Virginia Tech, Blacksburg, Virginia 24061, USA

²Department of Physics, Virginia Tech, Blacksburg, Virginia 24061, USA

*Email: metzmanj@vt.edu ; rheflin@vt.edu

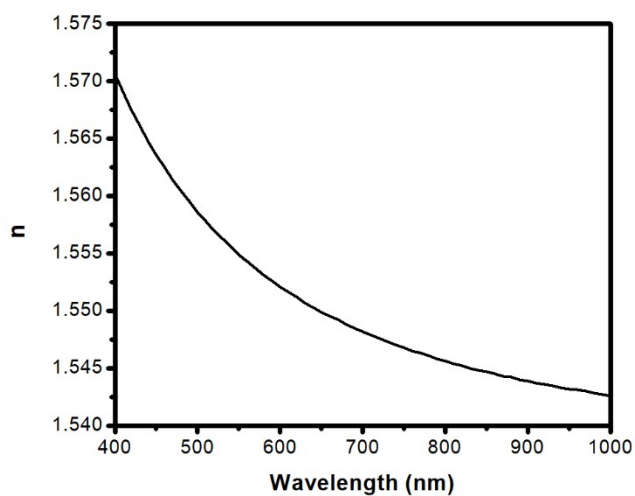


Figure S1. PAH/PAA refractive index vs. wavelength. Based on Cauchy dispersion model with $A = 1.5373$, $B = 0.0053271$, and $C = 0$.

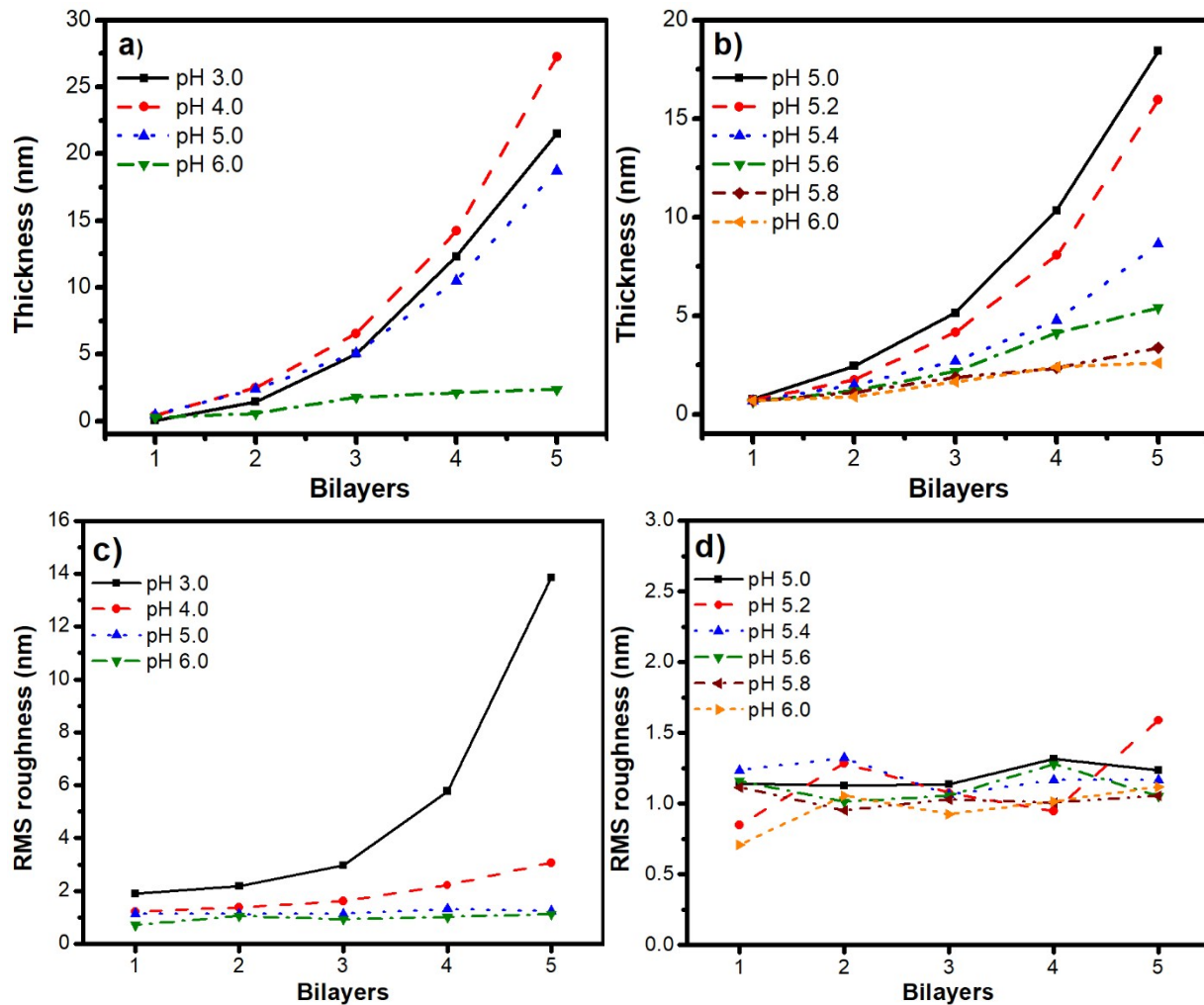


Figure S2. Thickness measurements for 1 to 5-bilayers of PAH_{7.0}/PAA_x films with (a) PAA_{3.0} to PAA_{6.0} and (b) PAA_{5.0} to PAA_{6.0}. RMS surface roughness measurements for 1 to 5-bilayers of PAH_{7.0}/PAA_x films for (c) PAA_{3.0} to PAA_{6.0} and (d) PAA_{5.0} to PAA_{6.0}.

PAA pH	y_0	a	b	R^2
3.0	-3.80	2.07	0.50	0.993
4.0	-2.56	1.59	0.59	0.999
5.0	-2.24	1.63	0.51	0.999
5.2	-1.17	0.78	0.62	0.999
5.4	-1.04	0.89	0.47	0.998
5.6	-3.87	3.17	0.22	0.977
5.8	-3.04	2.93	0.15	0.975
6.0	4.33	-5.10	-0.20	0.878

Figure S3. Exponential growth constants of Eq. (1) for PAH_{7,0}/PAA_x films with the PAA pH (x) range from 3.0 to 6.0. All of the exponential-growth thickness curves were modeled (with Origin Pro software) by a single-term exponential function of the form

$$y = y_0 + ae^{bx}$$

where a is the growth factor, b is the growth constant, and x is the number of bilayers. A coefficient of determination (R^2) was also reported with the model parameters, to show the effectiveness of the model in the representation of the data. This value comparatively signified how well the growth characteristics fit a single exponential.

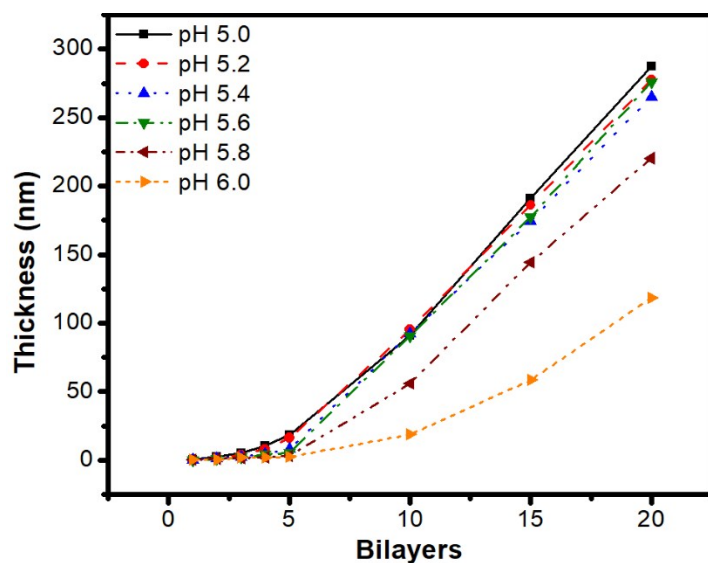


Figure S4. Thickness measurements for one to twenty bilayers of PAH_{7,0}/PAA_x films with PAA_{5,0} to PAA_{6,0}.

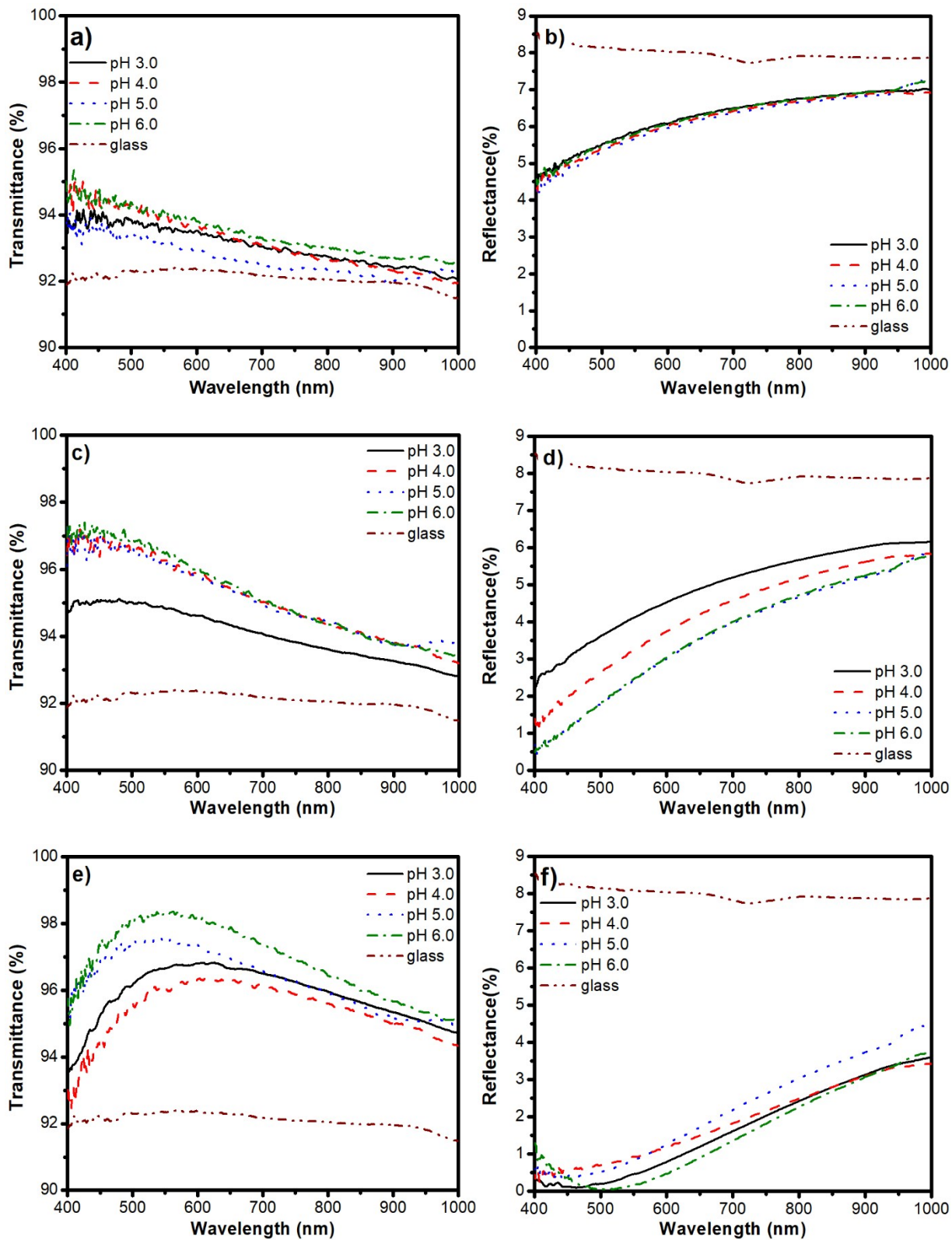


Figure S5. Measurements of (a) 1 quadlayer transmittance, (b) 1 quadlayer reflectance, (c) 2 quadlayer transmittance, (d) 2 quadlayer reflectance, (e) 3 quadlayer transmittance, (f) 3 quadlayer reflectance for interlayer ISAM ARC's of the architecture $[\text{PAH}_7/\text{PAA}_x/\text{PAH}_7/\text{SiO}_2]_{n=4.5}$ with PAA_x , x ranged from 3.0 to 6.0, by 1.0 increments. All of the films were thermally crosslinked at 200 °C for 2 hours.

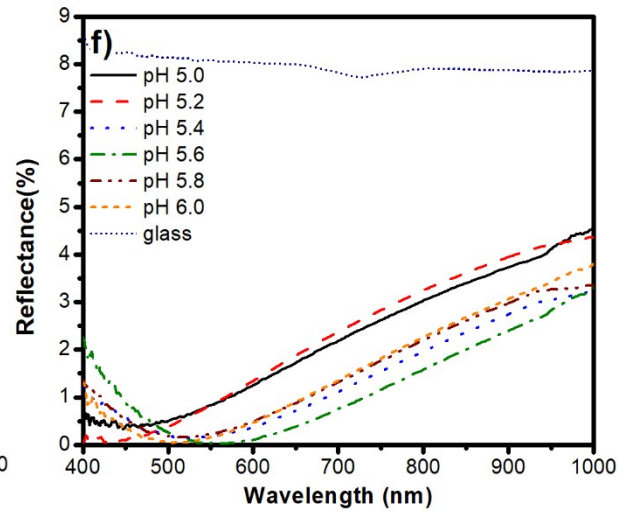
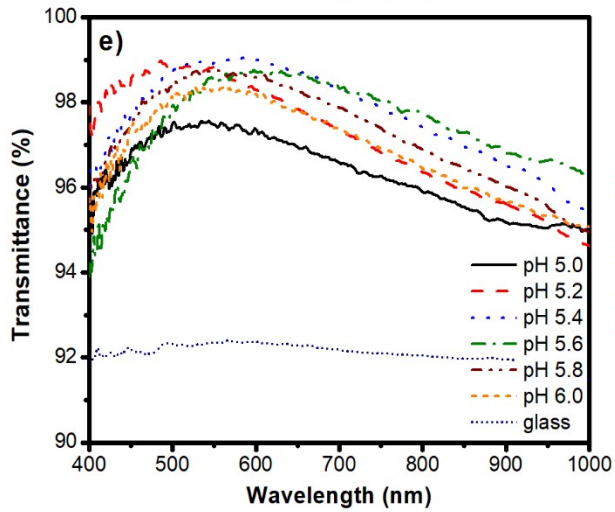
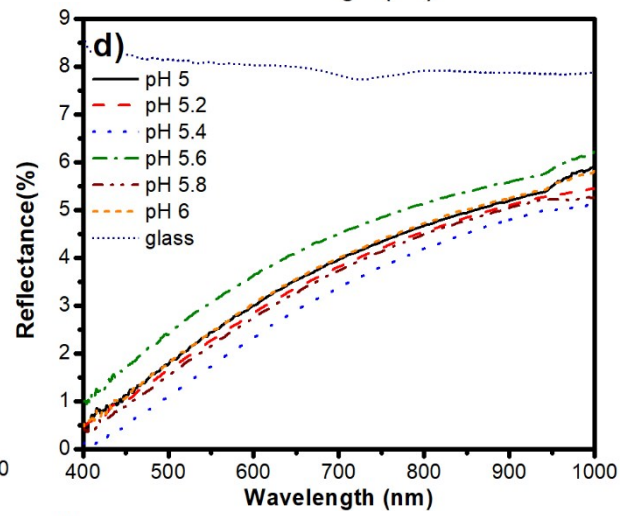
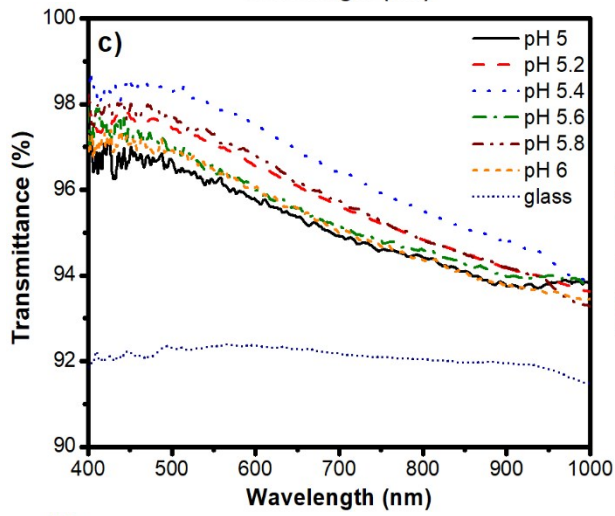
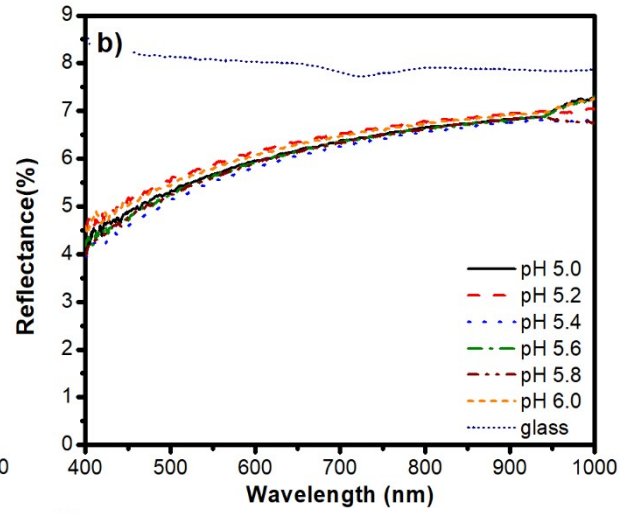
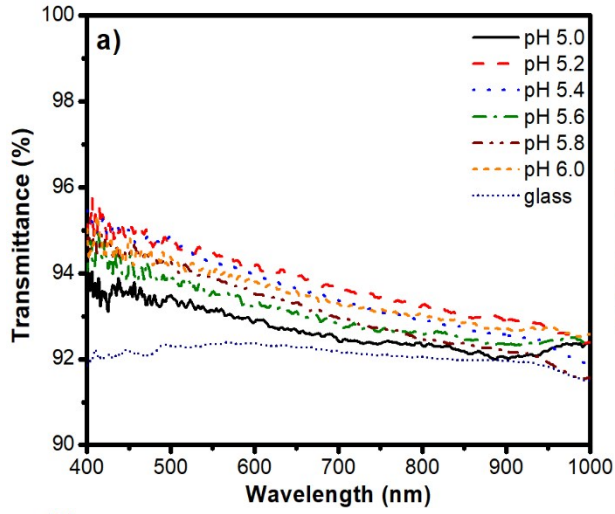


Figure S6. Measurements of (a) 1 quadlayer transmittance, (b) 1 quadlayer reflectance, (c) 2 quadlayer transmittance, (d) 2 quadlayer reflectance, (e) 3 quadlayer transmittance, (f) 3 quadlayer reflectance for interlayer ISAM ARC's of the architecture $[\text{PAH}_7/\text{PAA}_x/\text{PAH}_7/\text{SiO}_2]_{n=4.5}$ with PAA_x , x ranged from 5.0 to 6.0, by 0.2 increments. All of the films were thermally crosslinked at 200 °C for 2 hours.

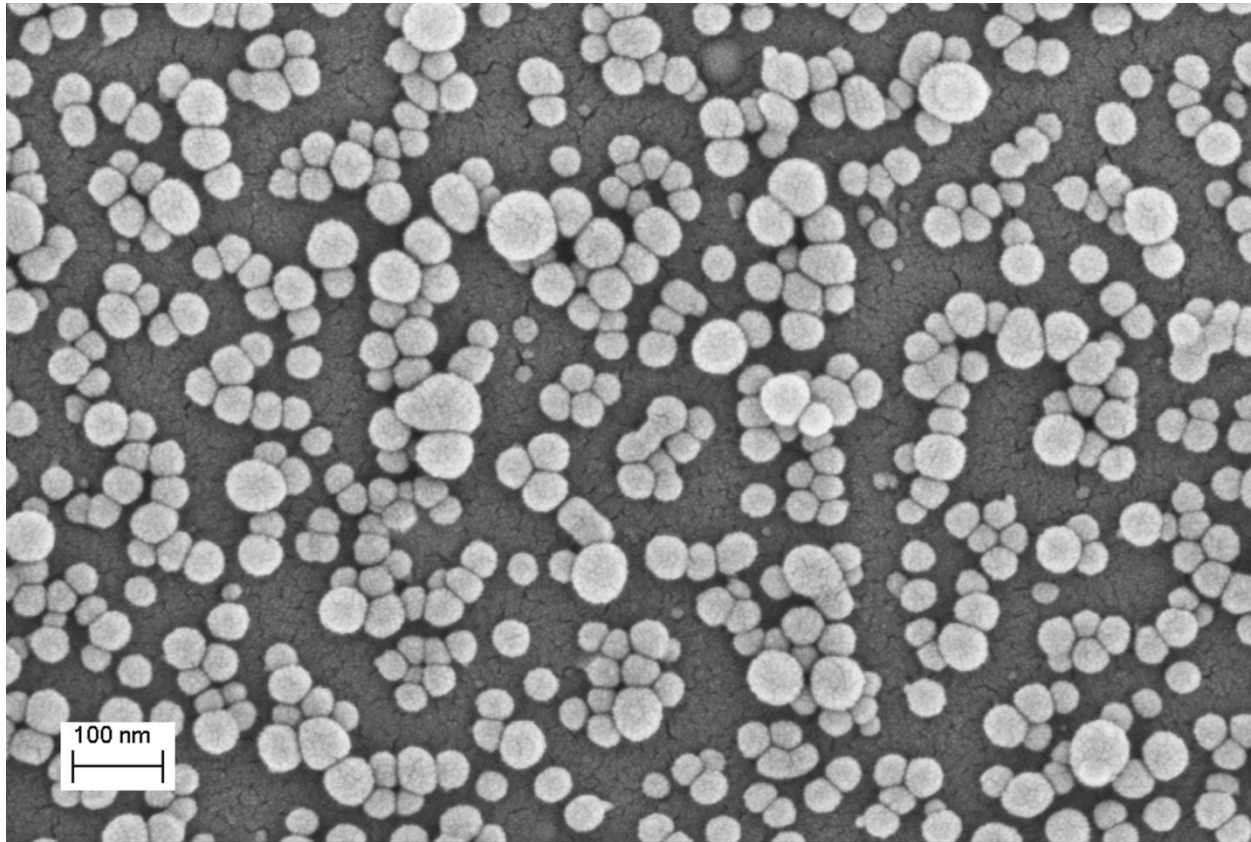
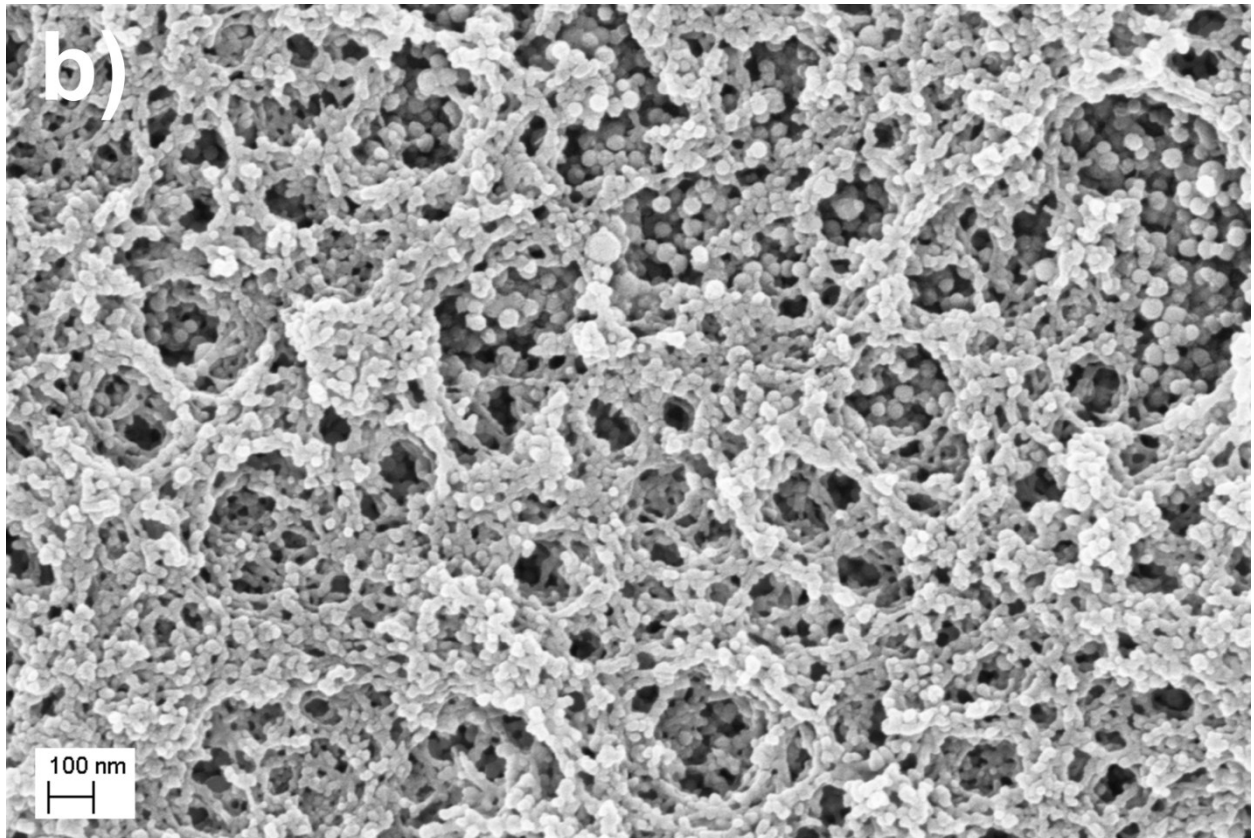
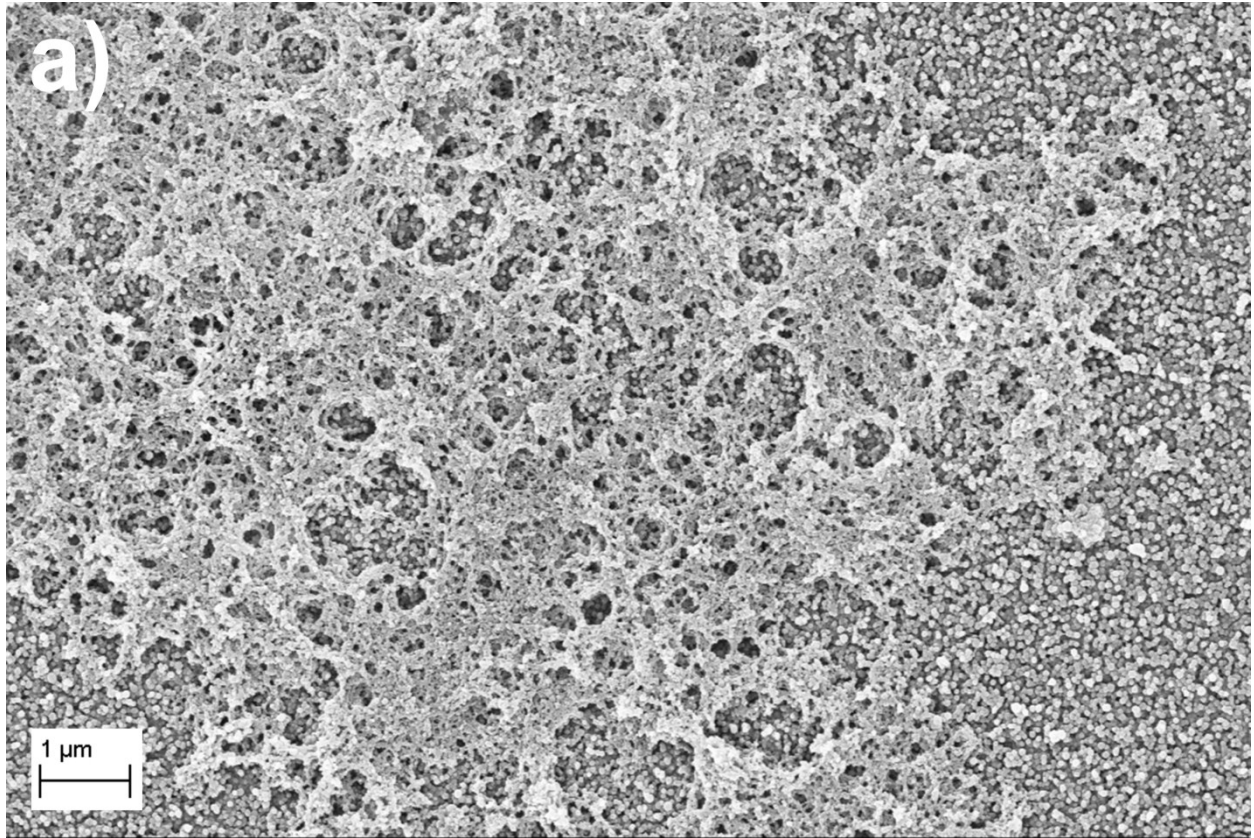


Figure S7. FESEM characterization 200 kX for a 1 quadlayer $[\text{PAH}_7/\text{PAA}_6/\text{PAH}_7/\text{SiO}_2]_{n=1.5}$ film. This film was thermally crosslinked at 200 °C for two hours.



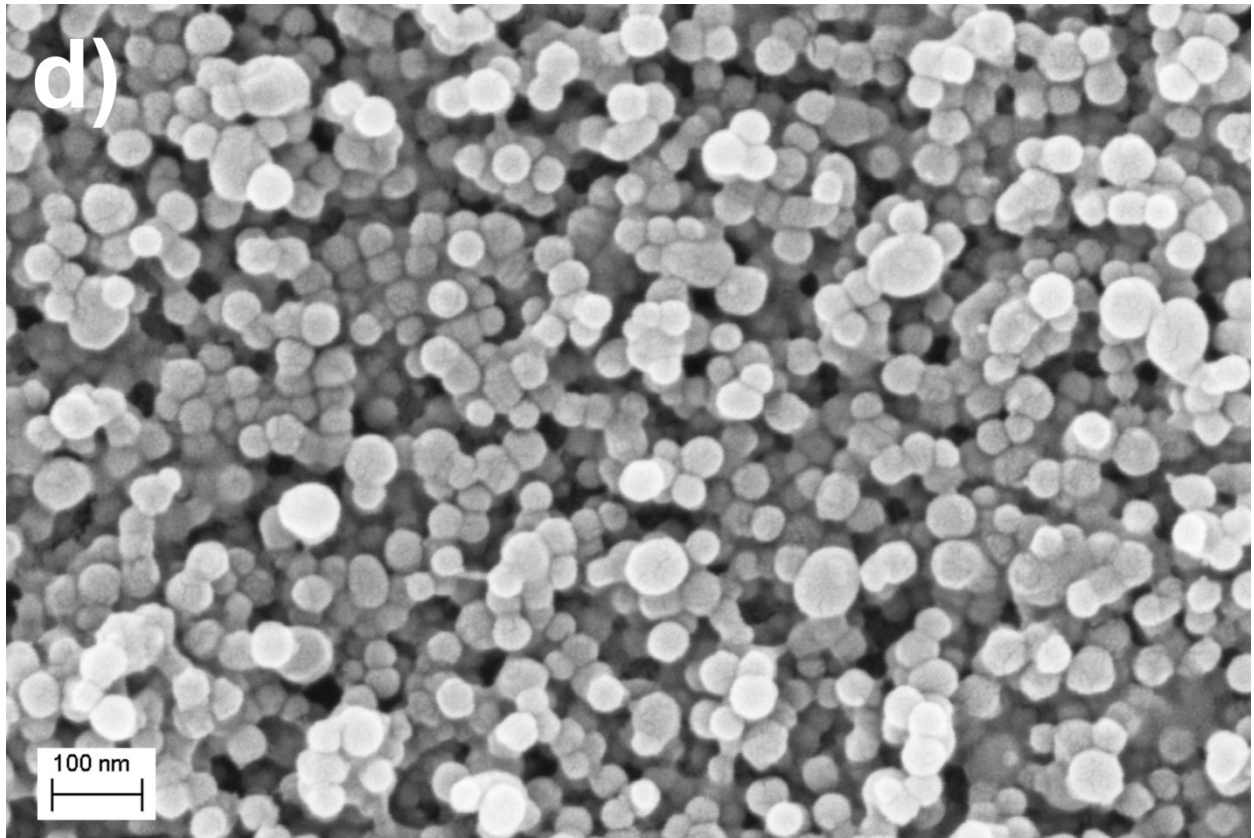
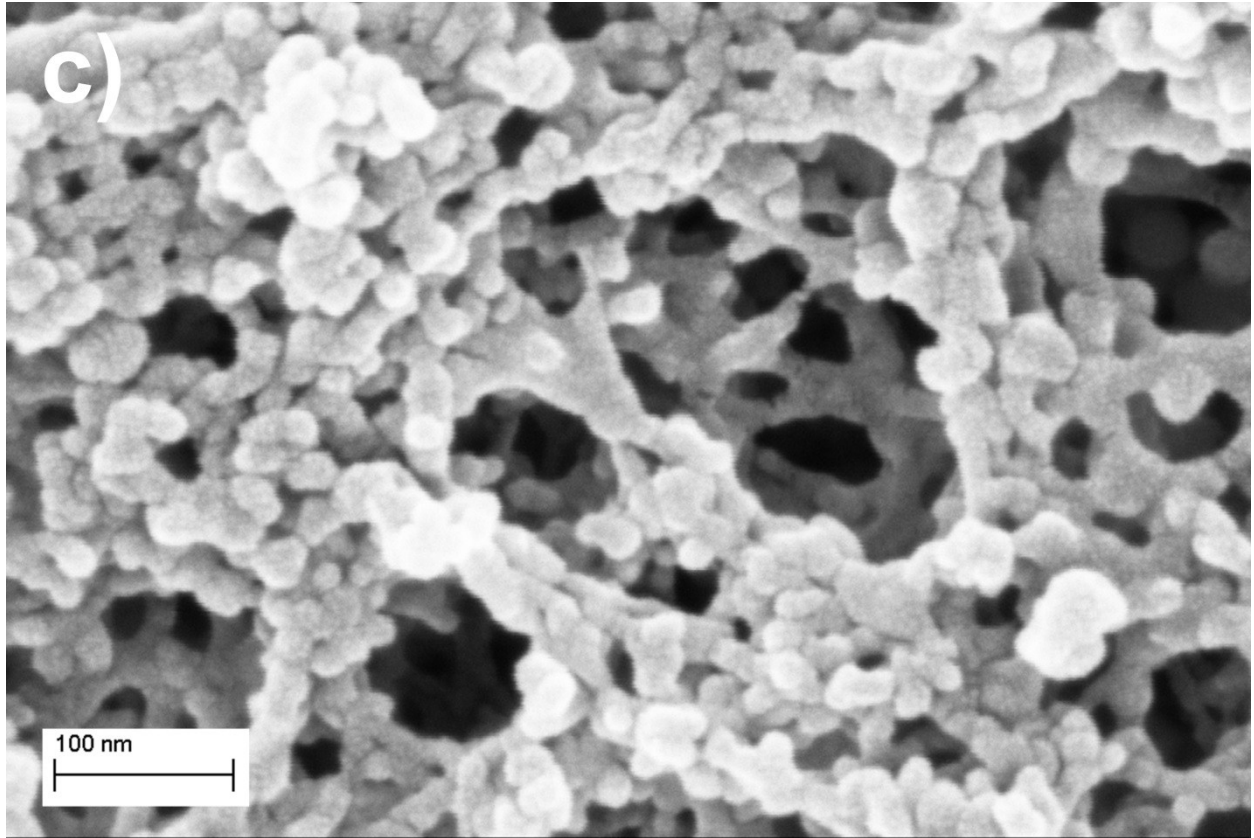


Figure S8. FESEM characterization for 4 quadlayer $[\text{PAH}_{7.0}/\text{PAA}_{3.0}/\text{PAH}_{7.0}/\text{SiO}_{2.9.0}]_{n=4.5}$ films, focused on the microporous formation for magnifications of (a) 20 kX, (b) 100 kX, (c) 400 kX. Images were also taken not focused on the microporous formations in the film at (d) 200 kX. All films were thermally crosslinked at 200 °C for two hours.

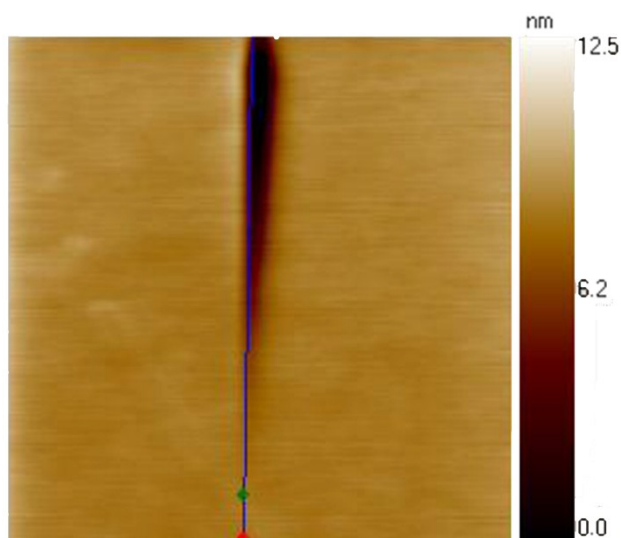


Figure S9. *In-situ* SPM characterization of a 10-bilayer $\text{PAH}_{7.0}/\text{PAA}_{7.0}$ film scratched up 1000 μN .